View metadata, citation and similar papers at core.ac.uk
brought to you by CORE
provided by MURAL - Maynooth University Research Archive Library

PHYSICAL REVIEW D **79,** 065036 (2009)

Non-Abelian Chern-Simons-Higgs solutions in 2 + 1 dimensions

Francisco Navarro-Lérida,[1] Eugen Radu,[2] and D. H. Tchrakian[3,4]

[1]*Departamento de Física Atómica, Molecular y Nuclear, Ciencias Físicas, Universidad Complutense de Madrid, E-28040 Madrid, Spain*

[2]*Institut für Physik, Universität Oldenburg, Postfach 2503, D-26111 Oldenburg, Germany*

[3]*School of Theoretical Physics, Dublin Institute for Advanced Studies, 10 Burlington Road, Dublin 4, Ireland*

[4]*Department of Computer Science, NUI Maynooth, Maynooth, Ireland*

(Received 12 December 2008; published 30 March 2009)

Non-Abelian vortices of an $SU(2)$ Chern-Simons-Higgs theory in 2 + 1 dimensions are constructed numerically. They represent natural counterparts of the $U(1)$ solutions considered by Hong, Kim, and Pac, and by Jackiw and Weinberg. The Abelian embeddings are identified, for all values of the Higgs self-interaction strength ν, resulting in both attractive and repulsive phases. A detailed analysis of the properties of the solutions reveals the existence of a number of unexpected features. For a certain range of the parameter ν, it is shown that the non-Abelian vortices have lower energy than their topologically stable Abelian counterparts The angular momentum of these vortices is analyzed and it is found that unlike the Abelian ones, whose angular momentum and energy are unrelated, there is a nontrivial mass-spin relation of the non-Abelian vortices.

DOI: 10.1103/PhysRevD.79.065036 PACS numbers: 11.15.−q, 11.10.Kk, 11.15.Kc

I. INTRODUCTION

Self-dual Abelian Chern-Simons-Higgs (CS-H) vortices were constructed by Hong, Kim, and Pac [1], and by Jackiw and Weinberg [2] describing anyonic solitons in 2 + 1 dimensions. These excited considerable interest because of their relevance to high T_c superconductivity and resulted in the development of a large body of literature, including also the case when the Maxwell term was present. For a complete review we refer to [3] (see also the recent work [4]). Soon after [1,2] appeared, the nonrelativistic counterpart[1] of that model was studied [5], followed by the non-Abelian versions of the latter, in [6,7]. The focus of the work on these nonrelativistic solitons is their relevance to integrable systems. The present work is concerned exclusively with the relativistic model.

The study of these Abelian CS-H vortices was motivated by the discovery in [8] of topologically massive (non-Abelian) Yang-Mills (YM) theories augmented by a Chern-Simons (CS) term. Thus it is that even before the discovery of the former [1,2], their non-Abelian versions were considered. Early work employing a non-Abelian Yang-Mills-CS-H (YM-CS-H) model featuring a pair of Higgs fields in the adjoint representations of $SU(2)$ was carried out in [9,10] and in the adjoint representations of $SU(N)$ in [11]. Non-Abelian CS-H vortices with Higgs field in the fundamental representation of $SU(2)$ were also discussed in [12]. Recently solutions in a supersymmetric $\mathcal{N} = 2$ non-Abelian CS-Higgs (CS-H) theory were considered in [13], and more recently, vortex solutions to a $U(N)$ YM-CS-H system with adjoint representation Higgs, describing the bosonic sector of a $\mathcal{N} = 2$ supersymmetric model, were given in [14] where the moduli space approach of [15] was employed to study the vortex dynamics at low energy.

To put our work in a larger context it should be remembered that non-Abelian vortices with a particular topology different from the one here are constructed in various gauged Higgs models. (Mostly the YM connection in these models enters via the usual quadratic YM term, but also in some examples both this and the CS term. These choices are irrelevant since the topology applied is insensitive to these dynamical details.) In contrast to our model and like that of [9], these models feature at least two adjoint representation Higgs fields in addition to other scalar multiplets, depending on the supersymmetry content. The most prominent feature of these non-Abelian vortices is that they are stabilized by Z_2 topology for gauge group $SU(2)$, and more generally they are the Z_N strings for gauge group $SU(N)$. Exhaustive references to these works are given in the review [16]. From the viewpoint of physical application these strings have played a prominent role, describing flux tubes starting and ending on *confined monopoles*, in the context of dual confinement theory. In an important recent development genuinely non-Abelian vortices in certain $\mathcal{N} = 2$ supersymmetric gauge theories were constructed in [16–20].

Unlike the previous models supporting non-Abelian Z_N vortices, the model employed in the present work has only one adjoint Higgs field and one $SU(2)$ gauge group and no supersymmetry. Moreover, the solutions constructed do not have Z_2 topology. It is the simplest possible $SU(2)$ extension of the 2 + 1 dimensional Abelian CS-H model of [1,2], with adjoint representation Higgs. The Abelian em-

[1]These gauged Schrödinger equations are not precisely the nonrelatitivistic limits of the ones considered here since they do not involve a symmetry breaking self-interaction potential of the scalar field.

 © 2009 The American Physical Society

bedding of these $SU(2)$ vortices in the self-dual limit are none other than the self-dual vortices of [1,2]. Thus our solutions have no relevance to dual confinement in QCD as the Z_N vortices do. Any relevance they have could be in condensed matter physics, but our emphasis here is exclusively on the analytic and numerical study of these solutions and not on their physical application. Another aspect in which our vortices differ from those studied to date is that in the existing literature on this subject no numerical constructions of non-Abelian CS-H vortices are presented. Given the absence of analytic solutions in closed form, the numerical analysis of this system is the pertinent one.

The only topological charge relevant to our purposes is the vortex number, pertaining exclusively to the embedded Abelian subsystem. Therefore we expect that the non-Abelian solutions we find are generically unstable. In fact they are sphaleronlike configurations with directions of instability. Some of these may decay into *unit* vorticity Z_2 Abelian vortices since our gauge group is $SU(2)/Z_2$ and $\pi_1(SU(2)/Z_2) = Z_2$. Not unexpectedly the non-Abelian solutions we find bifurcate from the corresponding Abelian embedding vortex, and interestingly, the non-Abelian vortex has lower energy than the Abelian one for certain parameter ranges.

Another interesting question we addressed is that of the value of the angular momentum of the non-Abelian vortices, which is the only global quantity exclusively characterizing these, relative to the known values for their Abelian counterparts [1,2].

Finally, as a byproduct of the present work we have constructed the non-self-dual version of the Abelian solutions of [1,2] by departing from the Bogomol'nyi limit away from the critical value of the Higgs self-interaction strength. (Surprisingly, no such analysis seems to have appeared to date.) The resulting solutions exhibit the same properties of mutual attraction and repulsion that are seen in the usual Abelian Higgs model itself [21]. It appears that to date this particular result has not appeared in the literature. After constructing these Abelian vortices, we proceed to construct the fully non-Abelian solutions, both for the value of the Higgs self-interaction parameter for which the Abelian embedding is self-dual and for other values of this parameter.

The paper is structured as follows: in the next section we present the model, impose rotational symmetry, and discuss the residual one-dimensional system. Then in Sec. III we carry out the numerical constructions and summarize our results in Sec. IV.

II. THE MODEL

A. The action and the general Ansatz

The CS-Higgs model on a $2+1$ dimensional Minkowski spacetime is described by the following Lagrangian:

$$\mathcal{L} = \Omega_{\rm CS} + \mathrm{Tr}\, D_\mu \Phi D^\mu \Phi - V(|\Phi|, \eta) \tag{1}$$

in which the CS density is

$$\Omega_{\rm CS} = \frac{\kappa}{2}\varepsilon^{\rho\mu\nu}\,\mathrm{Tr}\, A_\rho\left(F_{\mu\nu} - \frac{2}{3}A_\mu A_\nu\right), \tag{2}$$

and the symmetry breaking Higgs self-interaction potential is that employed in [1,2]

$$V = (4\lambda)^2\,\mathrm{Tr}\,\Phi^2(\eta^2 + \Phi^2)^2. \tag{3}$$

The dimensions of the various constants appearing above are $[\eta] = L^{-1}$, $[\lambda] = L$, and $[\kappa] = L^{-1}$ and the index $\mu = 0, i$, with $i = 1, 2$. The Lagrangian (1) usually enters the more complicated models as the basic building block (see e.g. [14] and the references therein). Therefore one can expect the basic features of its solutions to be generic.

The static Hamiltonian of the Lagrangian (1) is

$$\begin{aligned}\mathcal{H}_{\rm stat} &= \tfrac{1}{2}[\mathrm{Tr}(D_0\Phi^2 + D_i\Phi^2) + V(|\Phi|, \eta)] \\ &= \tfrac{1}{2}[\mathrm{Tr}([A_0, \Phi]^2 + D_i\Phi^2) + V(|\Phi|, \eta)].\end{aligned} \tag{4}$$

We take the static "spherically" symmetric $SO(4)$ YM field in three spacetime (i.e. two Euclidean) dimensions, in one or another chiral representation of $SO_\pm(4)$, such that our Ansatz is expressed in terms of the representation matrices

$$\Sigma^{(\pm)}_{\alpha\beta} = -\frac{1}{4}\left(\frac{1 \pm \gamma_5}{2}\right)[\gamma_\alpha, \gamma_\beta], \qquad \alpha, \beta = 1, 2, 3, 4, \tag{5}$$

$\gamma_\alpha = (\gamma_i, \gamma_M)$, with the index $M = 3, 4$ being the gamma matrices in four dimensions and γ_5, the chiral matrix.

Our rotationally symmetric Ansatz for the Higgs field Φ and the YM connection $A_\mu = (A_0, A_i)$ is

$$\begin{aligned}\Phi &= -(\varepsilon\phi)^M n_j \Sigma^{(\pm)}_{jM} - \phi^5 \Sigma^{(\pm)}_{34}, \\ A_0 &= -(\varepsilon\chi)^M n_j \Sigma^{(\pm)}_{jM} - \chi^5 \Sigma^{(\pm)}_{34}, \\ A_i &= \left[\left(\frac{\xi^M}{r}\right)(\varepsilon\hat{x})_i(\varepsilon n)_j + (\varepsilon A_r)^M \hat{x}_i n_j\right]\Sigma^{(\pm)}_{jM} \\ &\quad + \left[A^5_r \hat{x}_i + \left(\frac{\xi^5 + n}{r}\right)(\varepsilon\hat{x})_i\right]\Sigma^{(\pm)}_{34},\end{aligned} \tag{6}$$

in which the functions $(\xi^M, \xi^5) \equiv \vec{\xi}$, $(\chi^M, \chi^5) \equiv \vec{\chi}$, and $(A^M_r, A^5_r) \equiv \vec{A}_r$ parametrize the YM connection in terms of three sets of isotriplets $\vec{\xi}$, $\vec{\chi}$, and $\vec{A}_r$, the isotriplet $(\phi^M, \phi^5) \equiv \vec{\phi}$ parametrizing the Higgs field. All four isotriplets depend only on the two-dimensional spacelike radial variable r, ε is the two dimensional Levi-Civita symbol, and $n_i = (\cos n\varphi, \sin n\varphi)$ is the unit vector encoded with the winding (vortex) number $n \geq 1$ in the (x_1, x_2) plane (with $r^2 = x_1^2 + x_2^2$).

Having stated the Ansatz (6) in terms of the gamma matrices in four dimensions, we adopt henceforth the simpler labeling $\vec{\xi} = (\xi^M, \xi^3)$, $\vec{\chi} = (\chi^M, \chi^3)$, $\vec{\phi} = (\phi^M, \phi^3)$, and $\vec{A}_r = (A^M_r, A^3_r)$, with $M = 1, 2$ now.

B. The residual system and a consistent truncation

The parametrization used in (6) results in $SO(3)$ gauge covariant expressions for the YM curvature $F_{\mu\nu} = (F_{ij}, F_{i0})$ and the components of the covariant derivative of the Higgs field $D_\mu\Phi = (D_i\Phi, D_0\Phi)$, expressed exclusively in terms of the covariant derivatives of the three triplets $\vec{\xi} = (\xi^M, \xi^3)$, $\vec{\chi} = (\chi^M, \chi^3)$, and $\vec{\phi} = (\phi^M, \phi^3)$, these covariant derivatives in the residual one-dimensional space being defined as

$$\begin{aligned} D_r\xi^a &= \partial_r\xi^a + \varepsilon^{abc}A_r^b\xi^c, \\ D_r\chi^a &= \partial_r\chi^a + \varepsilon^{abc}A_r^b\chi^c, \\ D_r\phi^a &= \partial_r\phi^a + \varepsilon^{abc}A_r^b\phi^c. \end{aligned} \tag{7}$$

That the residual one-dimensional system of fields resulting from the imposition of this symmetry is entirely expressed in terms of the $SO(3)$ covariant quantities (7) is a consequence of the consistency of the Ansatz (6), which has been verified explicitly.

The Euler-Lagrange equations arising from the variation of the gauge field are

$$\begin{aligned} \frac{\kappa}{2}\varepsilon_{ij}F_{ij} + [\Phi, [A_0, \Phi]] &= 0, \\ \kappa\varepsilon_{ij}F_{j0} - [\Phi, D_i\Phi] &= 0, \end{aligned} \tag{8}$$

the first of which being the Gauss law equation. The Higgs equation is

$$D_iD_i\Phi - [A_0, [A_0, \Phi]] - \lambda\eta^2\Phi(\eta^2 + \Phi^2)(\eta^2 + 3\Phi^2) = 0. \tag{9}$$

With the notation (7), the gauge field equations (8) reduce to the following set of ordinary differential equations:

$$\begin{aligned} \frac{\kappa}{2r}D_r\vec{\xi} &= -[|\vec{\phi}|^2\vec{\chi} - (\vec{\phi}.\vec{\chi})\vec{\phi}], \\ \frac{\kappa r}{2}D_r\vec{\chi} &= -[|\vec{\phi}|^2\vec{\xi} - (\vec{\phi}.\vec{\xi})\vec{\phi}], \end{aligned} \tag{10}$$

together with the constraint equation

$$\vec{\phi} \times D_r\vec{\phi} = \frac{\kappa}{2r}\vec{\xi} \times \vec{\chi}. \tag{11}$$

The Higgs equation reduces to

$$\begin{aligned} D_r(rD_r\vec{\phi}) - \frac{1}{r}[|\vec{\xi}|^2\vec{\phi} - (\vec{\phi}.\vec{\xi})\vec{\xi}] + r[|\vec{\chi}|^2\vec{\phi} - (\vec{\phi}.\vec{\chi})\vec{\chi}] \\ - \lambda^2 r(\upsilon^2 - |\vec{\phi}|^2)(\upsilon^2 - 3|\vec{\phi}|^2)\vec{\phi} = 0. \end{aligned} \tag{12}$$

In (12), we have rescaled the vacuum expectation value (VEV) η as $\eta = \frac{1}{2}\upsilon$ to simplify the expression. We note that the winding number n in the Ansatz does not appear explicitly in the equations of motion (10) and (12), nor in the constraint equation (11). It will appear only in the boundary value of the function ξ^3 at the origin.

That (11) is a constraint equation is easily verified by acting on it with D_r and employing the other three field equations. In what follows we shall set the triplet of functions $\vec{A}_r = 0$, removing some of the $SO(3)$ gauge degeneracy in the residual system. That this is a consistent truncation is obvious since there is no curvature in one dimension.

Substituting (6) in (1) yields the following reduced one-dimensional Lagrangian:

$$\begin{aligned} L = \frac{\kappa}{2}[\vec{\chi}\cdot\vec{\xi}_r - (\vec{\xi}\cdot\vec{\chi}_r + n\chi_r^3)] + r|\vec{\phi}\times\vec{\chi}|^2 \\ - \left(r|\vec{\phi}_r|^2 + \frac{1}{r}|\vec{\phi}\times\vec{\xi}|^2\right) - \lambda^2 r|\vec{\phi}|^2(\upsilon^2 - |\vec{\phi}|^2)^2. \end{aligned} \tag{13}$$

The equations of motion (10) and (12), with all covariant derivatives replaced by the ordinary derivatives $D_r\vec{\phi} \to \frac{d\vec{\phi}}{dr} \equiv \vec{\phi}_r$, etc., follow from the variation of (13) with respect to the three triplets $\vec{\chi}$, $\vec{\xi}$, and $\vec{\phi}$, respectively.

It turns out that the Ansatz (6) can be consistently truncated further by setting

$$\vec{\xi} = (ck^M, a), \qquad \vec{\chi} = (dk^M, b), \qquad \vec{\phi} = (\upsilon hk^M, \upsilon g), \tag{14}$$

where k^M is a constant *unit length* 2-vector.[2] We are thus left with only six radial functions $a(r)$, $b(r)$, $c(r)$, $d(r)$, $h(r)$, and $g(r)$ resulting in the truncated version of the reduced Lagrangian (13)

$$\begin{aligned} L_{\text{trunc}} = -\frac{\kappa}{2}[(ab_r - ba_r) + (cd_r - dc_r) + nb_r] \\ + \upsilon^2 r(bh - dg)^2 - \upsilon^2\Big[r(h_r^2 + g_r^2) + \frac{1}{r}(ah - cg)^2 \\ + \upsilon^4\lambda^2 r(h^2 + g^2)[1 - (h^2 + g^2)]^2\Big] \end{aligned} \tag{15}$$

leading to the static energy density functional resulting from (15)

$$\begin{aligned} H_{\text{trunc}} = \frac{1}{2}\upsilon^2\Big[r(bh - dg)^2 + r(h_r^2 + g_r^2) + \frac{1}{r}(ah - cg)^2 \\ + \upsilon^4\lambda^2 r(h^2 + g^2)[1 - (h^2 + g^2)]^2\Big]. \end{aligned} \tag{16}$$

C. The Abelian case

It is natural at this stage to isolate the Abelian embedding of this system, which will play an essential role in the construction of the non-Abelian solutions. The Abelian embedding results from the truncation

$$c = d = g = 0,$$

for which the constraint (11) is identically satisfied.

[2]Using different constant *unit length* 2-vectors in $\vec{\xi}$, $\vec{\chi}$, and $\vec{\phi}$ does not lead to a consistent truncation.

The remarkable feature of this Abelian case is that the Gauss law equation is an algebraic equation enabling the elimination of the electric component A_0 of the Maxwell field $A_\mu = (A_i, A_0)$. This results in the reduction of the static Hamiltonian becoming identical with that of the usual Abelian Higgs model, subject to an additional *proviso* restricting the symmetry breaking Higgs self-interaction potential to be of the form (3), namely, the natural case chosen in [1,2].

The Gauss law equation now reduces to

$$b = -\frac{\kappa}{2v^2h^2}\frac{a_r}{r}, \tag{17}$$

leading to the reduced one-dimensional Lagrangian

$$L_{U(1)} = \frac{\kappa}{2}[ba_r - (a+1)b_r] + v^2rb^2h^2 - v^2\left(rh_r^2 + \frac{a^2h^2}{r}\right) - \lambda^2v^6rh^2(1-h^2)^2. \tag{18}$$

The Gauss Law constraint (17) can now also be derived from the variation of (18) with respect to $b(r)$.

Next, using integration by parts, we replace the term $(a+1)b_r$ in (18) by ba_r, whence (18) can be expressed as

$$L_{U(1)} = -v^2\left\{\left[\frac{\kappa^2}{4v^4}\frac{a_r^2}{rh^2} + \lambda^2v^4rh^2(h^2-1)^2\right] + \left(rh_r^2 + \frac{a^2h^2}{r}\right)\right\} \equiv -H_{\text{stat}}. \tag{19}$$

To establish the topological lower bound of H_{stat} defined by (19), we consider the two inequalities

$$\left(\sqrt{r}h_r \mp \frac{ah}{\sqrt{r}}\right)^2 \geq 0,$$

$$\left[\frac{\kappa}{v^2}\frac{a_r}{2\sqrt{r}h} \mp \lambda v^2\sqrt{r}h(h^2-1)\right]^2 \geq 0,$$

which lead to the final inequality

$$H_{\text{stat}} \geq \pm v^2[a(h^2-1)_r + \kappa\lambda a_r(h^2-1)]. \tag{20}$$

Now for this inequality to present a topological lower bound on the energy, the right-hand side of (20) must be a total derivative. This is only possible if we choose the constants subject to

$$\kappa\lambda = 1. \tag{21}$$

Saturating (20) with (21) yields precisely the Bogomol'nyi equations satisfied by the self-dual Chern-Simons vortices of [1,2], which is relevant here because our numerical analysis will depart from these vortices, first to the non-self-dual case analogous to the corresponding Abelian Higgs vortices [21], and finally to the non-Abelian vortices.

D. The global charges

On the question of the magnetic and electric fluxes, the situation is as follows. For the generic Abelian case, the operative equations are the Maxwell equations, and of these the Gauss law equation is [2]

$$\nabla \cdot E - \kappa B = \rho, \tag{22}$$

where $E_i = F_{i0}$ and $B = F_{12} = \frac{1}{2}\varepsilon_{ij}F_{ij}$. The density ρ is the 0th component of the $U(1)$ current expressed in terms of the complex Higgs field such that its volume integral over d^2x is the electric flux. The volume integral of the divergence term $\nabla \cdot E$, after converting it to a "surface" (line) integral, vanishes. This can be seen readily from the results of the foregoing asymptotic analysis. As a result of the vanishing of $\nabla \cdot E$ in (22) for our model, it is clear that the magnetic flux $\int Bd^2x$ is inversely related to the electric flux.

The only topological charge in this system is the magnetic flux, and hence also the electric flux. These are defined in the context of the Abelian subsystem of the $SU(2)$ model at hand, and these respective charges are the only global quantities pertaining to the solutions studied. The non-Abelianness therefore has no influence in this sector. There is, however, the angular momentum, or the spin, of these solutions, which presents another global quantity characterizing our solutions. Unlike the magnetic and electric charges, however, which are not influenced by the non-Abelianness, the angular dependence is indeed dependent on the gauge group.

The angular momentum density is

$$\mathcal{J} = T_{\varphi 0} = (x\varepsilon)_i T_{i0} = (\hat{x}\varepsilon)_i r \,\text{Tr}\, D_i\Phi D_0\Phi, \tag{23}$$

which, for the fields subjected to the Ansatz (6), and further truncated according to (14), readily yields

$$\mathcal{J} = \tfrac{1}{2}v^2(\vec{\phi}\times\vec{\chi})\cdot(\vec{\phi}\times\vec{\xi}) = \tfrac{1}{2}v^2(ah-cg)(bh-dg). \tag{24}$$

Remarkably enough, the total angular momentum, which is given by the integral

$$J = 2\pi\int \mathcal{J} r dr, \tag{25}$$

can be expressed as a difference of two boundary integrals[3] (thus in this one-dimensional case it reduces to the integral of a total derivative). It follows from the field equations (8), that the integral (25) can be written as

$$J = -\kappa\frac{\pi}{2}\int_0^\infty \vec{\xi}\cdot D_r\vec{\xi}dr = -\kappa\frac{\pi}{4}(|\vec{\xi}(\infty)|^2 - |\vec{\xi}(0)|^2) = \kappa\frac{\pi}{4}(n^2 - p_1^2). \tag{26}$$

Note that p_1 appearing in (26) is an asymptotic parameter appearing in (30) below, and that the Abelian embedding

[3]A similar property of the total angular momentum has been noticed in 3 + 1 dimensions for various models with gauged fields, see e.g. [22] and the references there. However, in contrast to the model here, for all known $d = 4$ cases, the contribution to J of the inner boundary term vanishes.

solution is consistent with the value $p_1 = 0$ of this parameter. Thus in this limit, the expression (26) coincides with the angular momentum given in [1,2], i.e. $J = \kappa\pi n^2/4$, which holds for both self-dual and non-self-dual solutions. It is clear that the angular momentum of the non-Abelian vortices differs essentially from that of its Abelian counterparts and that it can only be evaluated numerically, which will be described in the following section.

We further define the energy of the solutions as the integral of (16), namely,

$$E = 2\pi \int r T_{00} dr = 2\pi \int H_{\text{trunc}} dr. \tag{27}$$

III. NUMERICAL RESULTS

A. General features

Although an analytic or approximate solution appears to be intractable here we present arguments for the existence of nontrivial solutions of the field equations (10)–(12).

For the full non-Abelian system the asymptotic expansion of the solutions near the origin that guarantees regularity and differentiability is

$$\begin{aligned}
a(r) &= -n - \frac{d_n^2}{4(n+1)}\left(2 + \frac{4b_0 h_h^2 \upsilon^2}{d_n^2 \kappa}\right) r^{2n+2} + O(r^{2n+4}),\\
b(r) &= b_0 + \frac{h_n^2 \upsilon^2}{\kappa} r^{2n} + O(r^{2n+2}),\\
c(r) &= -\frac{d_n}{(n+2)}\left(b_0 + \frac{d_n^2 \kappa}{2h_n^2 \upsilon^2}\right) r^{n+2} + O(r^{n+4}),\\
d(r) &= d_n r^n + O(r^{n+2}), \qquad h(r) = h_n r^n + O(r^{n+2}),\\
g(r) &= -\frac{d_n \kappa}{2h_n \upsilon^2} - \upsilon^2 \lambda^2 \frac{d_n \kappa}{8h_n}\left(1 - \frac{3d_n^2 \kappa^2}{4h_n^2 \upsilon^4}\right)\left(1 - \frac{d_n^2 \kappa^2}{4h_n^2 \upsilon^4}\right) r^2\\
&\quad + O(r^4).
\end{aligned} \tag{28}$$

All higher order terms in this expansion are fixed by the coefficients b_0, d_n, h_n. Thus, at the origin one uses the following set of boundary conditions:

$$\begin{aligned}
a|_{r=0} &= -n, \qquad \partial_r b|_{r=0} = 0,\\
c|_{r=0} &= d|_{r=0} = h|_{r=0} = 0, \qquad \partial_r g|_{r=0} = 0.
\end{aligned} \tag{29}$$

At infinity, the finite energy requirements impose

$$\begin{aligned}
g &= \cos\alpha, \qquad h = \sin\alpha, \qquad a = p_1 \cos\alpha,\\
c &= p_1 \sin\alpha, \qquad d = p_2 \sin\alpha, \qquad b = p_2 \cos\alpha,
\end{aligned} \tag{30}$$

where α, p_1, p_2 are arbitrary constants fixed by numerics. Physically, p_1 and p_2 correspond to the asymptotic amplitudes of the effective scalars $\vec{\chi}$ and $\vec{\xi}$, respectively, while α somehow characterizes the angle of the Higgs field with respect to the Abelian solution, since $\alpha = \pi/2$ in that limit.

Let us now concentrate on the numerical resolution of Eqs. (10) and (12), together with the constraint given by Eq. (11). In order to do so, we employ a collocation method for boundary-value ordinary differential equations,[4] equipped with an adaptive mesh selection procedure [23]. Typical mesh sizes include 10^3–10^4 points. The solutions have a relative accuracy of 10^{-7}.

It is worth noticing that Eqs. (10)–(12) may be rescaled by

$$b \to \frac{2\upsilon^2}{\kappa} b, \qquad d \to \frac{2\upsilon^2}{\kappa} d, \qquad r \to \frac{\kappa}{2\upsilon^2} r, \qquad \lambda \to \frac{\nu}{\kappa}, \tag{31}$$

such that dependence on κ and υ disappears, remaining just a dependence on ν, which encodes the Higgs self-coupling parameter. For that reason, without loss of generality, we will assume in what follows that $\kappa = 2\upsilon^2$ and $\upsilon = 1$ and λ will be rewritten as $\nu/2$. With this convention, the Abelian solutions approach the self-dual limit for $\nu = 1$. For numerical reasons we further introduce a compactified radial coordinate defined by $\bar{r} = r/(1 + r)$.

After a detailed analysis of the equations, one finds that for a fixed integer n and a nonvanishing real ν, the regular solutions to (10)–(12) depend on just one numerical free parameter. We have chosen it to be p_2 so the two remaining constants in (30), namely, p_1 and α, are not free but are given by numerics. For that reason, in our numerical scheme the boundary conditions at infinity were chosen to be

$$d - p_2 h = 0, \qquad bh - dg = 0, \qquad g^2 + h^2 = 1. \tag{32}$$

To summarize, the numerical solutions are constructed by using the boundary conditions (29) and (32) with the following input parameters: the winding number n, the Higgs self-coupling constant ν, and the asymptotic value p_2 of the electric non-Abelian potential.[5]

Our procedure to generate non-Abelian solutions in the $\{n, \nu, p_2\}$ parameter space was as follows: for fixed integer n, one starts from the corresponding self-dual Abelian solution ($\nu = 1$ and $p_2 = 0$), which corresponds to the solution in [1,2]; moving ν from 1 while keeping $p_2 = 0$ one generates non-self-dual Abelian solutions; moving p_2 from zero[6] while keeping $\nu = 1$ one generates non-Abelian solutions with $\nu = 1$; finally, the general solutions are found when moving both ν and p_2. Also, nontrivial solutions are likely to exist for any value of the winding

[4]Some of the solutions were also constructed by using a standard Runge-Kutta ordinary differential equation solver. In this approach we evaluate the initial conditions at $r = 10^{-5}$ for global tolerance 10^{-12}, adjusting for shooting parameters h_n, b_0 and integrating towards $r \to \infty$. We have noticed very good agreement between the results obtained with these two different methods. The accuracy of the solutions was also monitored by computing a virial relation satisfied by the system (15).

[5]It is interesting to remark that these are also the usual input parameters for the dyonic Yang-Mills-Higgs (YMH) solutions in 3 + 1 dimensions, see e.g. [24].

[6]As we will show later for large values of ν there are non-Abelian solutions with $p_2 = 0$ in addition to the Abelian ones.

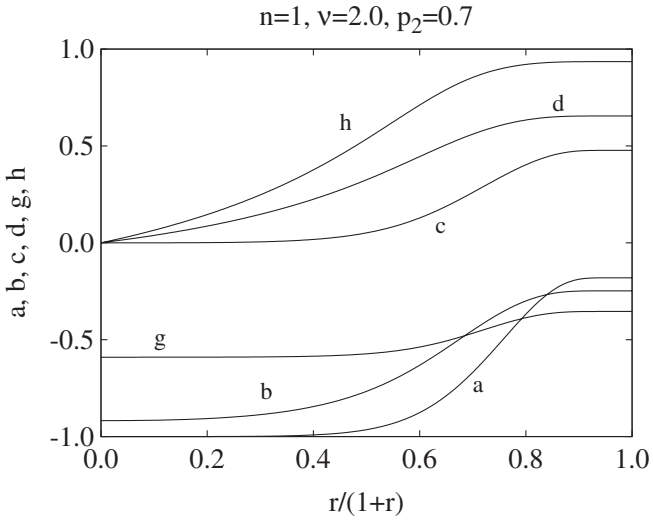

FIG. 1. A typical non-Abelian solution with $\nu = 2.0$ and $p_2 = 0.7$ is shown for $n = 1$.

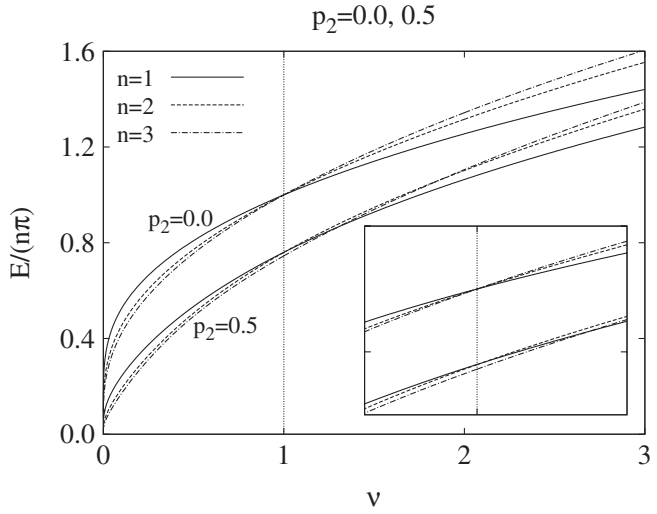

FIG. 2. Energy per vortex number E/n versus the Higgs self-coupling constant ν for Abelian ($p_2 = 0.0$) and non-Abelian ($p_2 = 0.5$) solutions with $n = 1, 2, 3$. In the Abelian case, the curves meet for $\nu = 1$, the self-dual limit.

number n; however, in practice, numerics becomes more involved with increasing n. Similarly, we have found non-Abelian solutions for arbitrarily large values of ν.

In Fig. 1 we show the functions a, b, c, d, g, and h for a typical non-Abelian solution (with $\nu = 2.0$ and $p_2 = 0.7$) for $n = 1$. The remarkable non-Abelian nature of these solutions is inferred from the significant deviation from zero of the functions c, d, and g.

B. The energy of the solutions

Let us analyze the energy of the solutions. In Fig. 2 we show the energy per vortex number of the Abelian solutions ($p_2 = 0$) versus ν for $n = 1, 2, 3$. In the self-dual limit ($\nu = 1$) the curves coincide. Below $\nu = 1$ the energy per vortex number decreases with n for fixed ν while above $\nu = 1$ it increases monotonically with n. This can be interpreted by saying that force between vortices is attractive below the self-dual limit ($\nu = 1$), while it is repulsive above $\nu = 1$. We also include for comparison the energy per vortex number of non-Abelian solutions with $p_2 = 0.5$. In that case there is no fixed self-dual limit where all the curves merge but curves cross in pairs at several values of ν.

The effect of non-Abelianity is exhibited in Figs. 3. In Fig. 3(a) the energy per vortex number is presented as a function of the parameter p_2 for several values of ν for $n = 1, 2, 3$. Starting from the corresponding Abelian solution ($p_2 = 0$) we move[7] p_2 for fixed n and ν. We observe numerically that solutions exist only in the range[8] $|p_2| \leq 1$.

When the limit $p_2 = \pm 1$ is approached the solution tends to the trivial solution

$$a = -n, \qquad b = -1, \qquad c = 0,$$
$$d = 0, \qquad g = \mp 1, \qquad h = 0. \tag{33}$$

This limit requires some explanation. When $|p_2| \to 1$ the sequence of solutions tends to (33) in a pointwise way. In fact, as we can see from Fig. 3(a) and subsequent ones, the energy for the limiting solution seems to depend on ν, and it is obviously nonvanishing. A naive computation of the energy using (33), however, yields zero. The explanation of this apparent contradiction may be understood by analyzing Fig. 4. There the energy density ($\varepsilon = 2\pi H_{\text{trunc}}$) of a sequence of solutions with $|p_2| \to 1$ is presented. We observe that the energy density spreads and tends to zero as $|p_2| \to 1$ but its integral remains finite. Moreover, if one concentrates on functions $\{a, b, c, d, g, h\}$ for the sequence, one observes that for any finite value of r the sequence tends to the corresponding limiting value although that is not necessarily true for the value at infinity.

For small values of ν we find only one solution for each value of p_2. However, for large values of ν we find several solutions for the same value of p_2 (the larger n is, the smaller ν needs to be) with a different value of the energy, in general. In Fig. 3(a) that is clearly seen for $n = 3$, $\nu = 2$ where in the range $0.63 < |p_2| < 0.75$ three different non-Abelian solutions coexist for each value of p_2.

Figures 3(b) and 3(c) show the energy per vortex number versus p_1 and α, respectively. It is clearly seen that the curves look much more complicated when using p_1 or α as a free parameter. Moreover, contrary to what happens when using p_2 as a free parameter, we do not observe any *a priori* bound for p_1 and α.

[7]Recall that the energy is an even function of p_2 and thus similar solutions exist when $p_2 \to -p_2$.

[8]Physically, that means the amplitude of the electric potential at infinity is always smaller than the asymptotic value of the Higgs field, a feature present also in 3 + 1 dimensional gauged Higgs models, see e.g. [24].

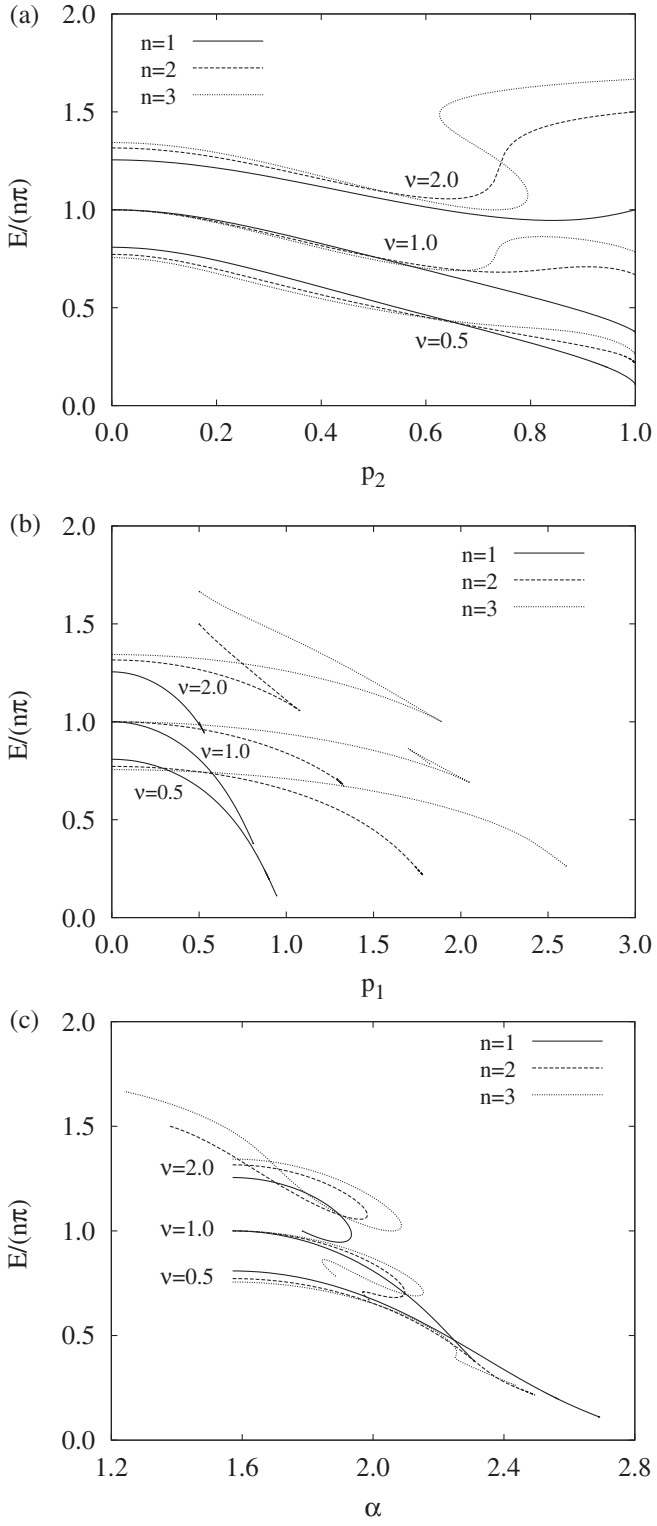

FIG. 3. (a) Energy per vortex number E/n versus the magnitude p_2 of the electric potential at infinity for solutions with $n = 1, 2, 3$ and several values of ν. For $\nu = 2$, $n = 3$, one notices the existence of several solutions with the same p_2. (b) Energy per vortex number E/n versus p_1 for solutions with $n = 1, 2, 3$ and several values of ν. (c) Energy per vortex number E/n versus α for solutions with $n = 1, 2, 3$ and several values of ν.

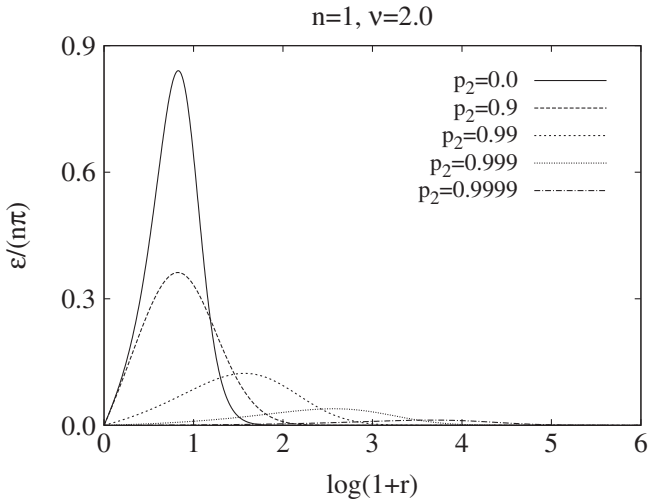

FIG. 4. Energy density ε for a sequence of solutions with $|p_2| \to 1$ for $n = 1$ and $\nu = 2.0$.

C. The angular momentum

The angular momentum of the solutions of Fig. 3(a) is exhibited in Fig. 5. Showing independence of ν for the Abelian case ($p_2 = 0$) we observe that the angular momenta of solutions with the same value of p_2 but different values of ν are different in general. As the masses of these solutions also change with changing p_2 it is useful to consider the behavior of the angular momentum as a function of the energy.

That is shown in Fig. 6. For small values of ν, the angular momentum J is an increasing function of the energy E. In fact, we observe that $J = 0$ solutions seem not to exist, except in the limit when the energy also vanishes. As ν is increased, the curves develop a kink but the angular momentum still remains to be an increasing function of the energy. However, as ν is enlarged more, one may find regions where the angular momentum becomes a decreasing function of the energy. Finally, for very large values of ν the angular momentum monotonically decreases with increasing energy. This strange effect has been reported previously in other theories (for instance, in $d = 3 + 1$ Einstein-Maxwell-dilaton theory [25], associated to counterrotation).

D. The issue of $p_2 = 0$ solutions

Unexpectedly, the multiplicity of solutions in p_2 we observe in Fig. 3(a) as a function of ν happens also at $p_2 = 0$ (although it cannot be seen there). Thus, the condition $p_2 = 0$ (i.e. $|\chi| \to 0$ as $r \to \infty$) does not characterize Abelian solutions.[9] These non-Abelian $p_2 = 0$ solutions exist for any value of the vorticity n. In Fig. 7 we show this

[9]This is a unique feature of $d = 2 + 1$ CS-H theories. In the better known $d = 4 + 1$ YMH case, $|A_0| = 0$ at infinity implies a vanishing electric potential.

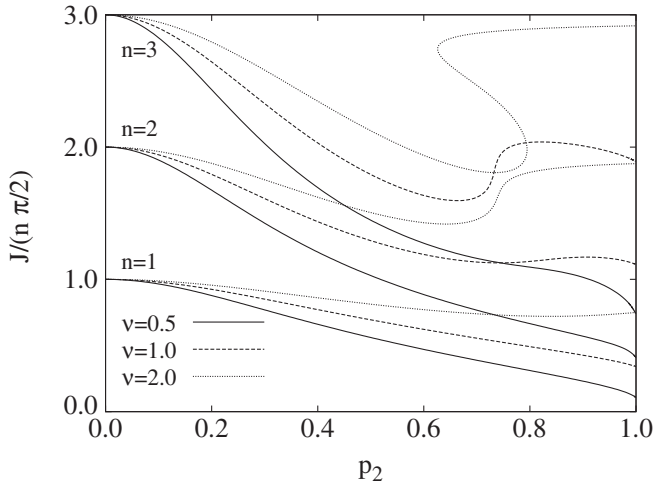

FIG. 5. Angular momentum per vortex number J/n versus p_2 for the same set of solutions as Fig. 3(a).

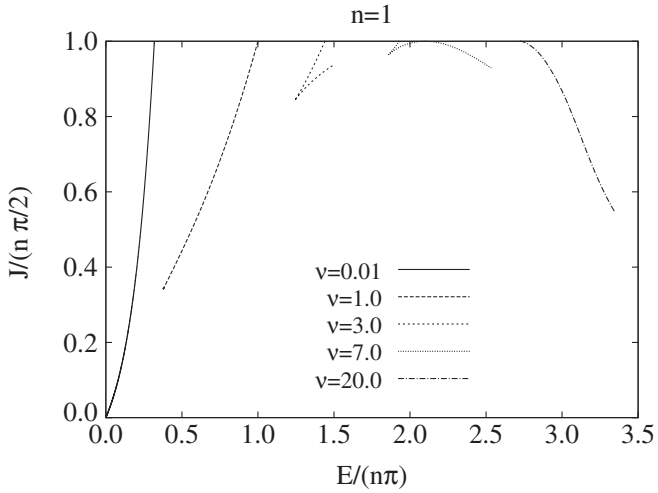

FIG. 6. Angular momentum per vortex number J/n versus energy per vortex number E/n for solutions with $n = 1$ and several values of ν.

for solutions with $n = 3$. It is clear how the curves get more complicated as ν increases with the appearance of non-Abelian $p_2 = 0$ solutions. Concerning Fig. 7 and the subsequent one Fig. 9, one should notice that only half of the complete curves are presented for the sake of clarity. Since the energy is an even function of p_2 the complete pictures would include also the mirror symmetric images, with respect to the $p_2 = 0$ line.

There is also one further feature one should mention. As a general rule, there are (almost always[10]) non-Abelian solutions with lower energy than the connected Abelian solution for fixed values of n and ν.

[10]We have observed, however, some small regions where that is not the case.

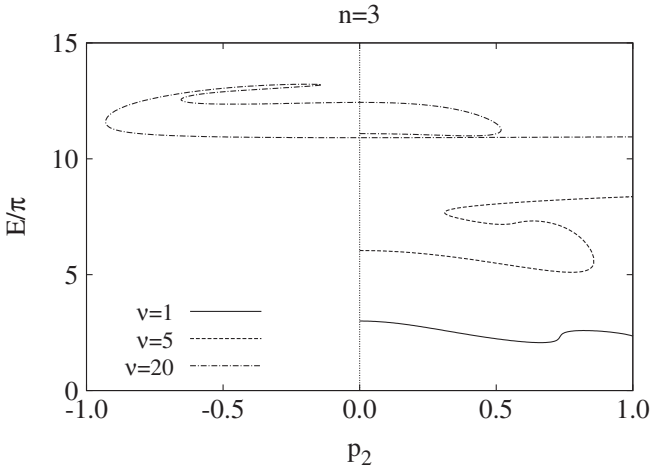

FIG. 7. Energy E versus p_2 for solutions with $n = 3$ and several values of ν.

Let us analyze further these $p_2 = 0$ solutions. In Fig. 8 we exhibit the energy E of $p_2 = 0$ solutions for $n = 1$. The picture is similar for any other value of n (although there are more kinks as n increases). Plotting the Abelian branch of solutions we observe there is a value of ν ($\nu \simeq 75.0$, 54.2, 55.6 for $n = 1$, 2, 3, respectively) at which the non-Abelian $p_2 = 0$ branch branches off (represented by a large dot in Fig. 8). Following the non-Abelian branch we observe it crosses the Abelian branch at another value of ν. That means it is possible to find two different solutions with the same values of $\{n, \nu, p_2, E\}$. Above that value we observe the existence of non-Abelian $p_2 = 0$ solutions with energy lower than the corresponding energy of their Abelian counterparts.

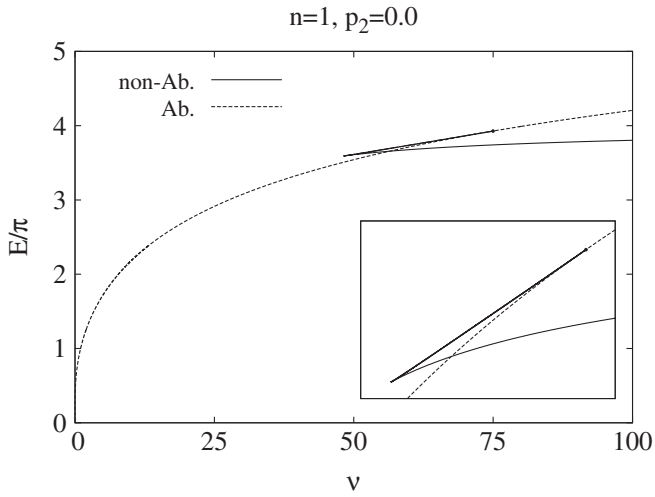

FIG. 8. Energy E versus the Higgs self-coupling parameter ν for $p_2 = 0$ solutions with $n = 1$. For a range of ν, the non-Abelian solutions have a lower energy than their Abelian counterparts.

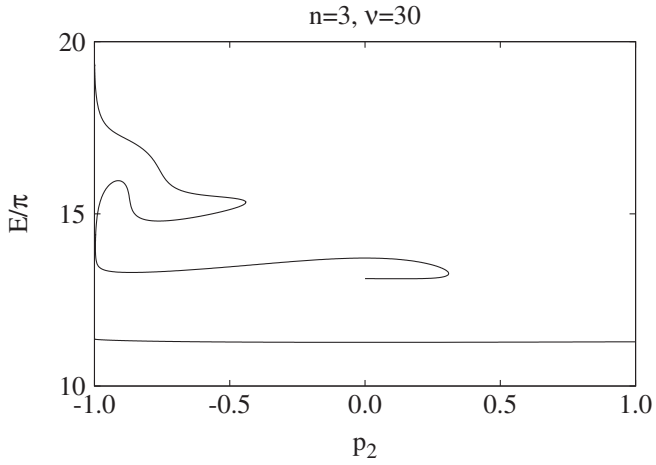

FIG. 9. Energy E versus p_2 for $n = 3$, $\nu = 30$ solutions. A branch disconnected from the Abelian solution (starting point at $p_2 = 0$) is shown.

E. Disconnected branches

Even more strange situations may happen for large values of the Higgs self-coupling constant ν. There we have found numerical evidence for the existence of disconnected non-Abelian branches. In general, all these non-Abelian solutions reported above are obtained by continuous variation of the free parameter p_2 in the range $|p_2| \leq 1$. However, by fine-tuning ν and p_2 it is possible to reach a region of the parameter space where the corresponding Abelian solution cannot be reached by just moving p_2, i.e., one can move p_2 from -1 to 1 (passing through 0) without reaching the Abelian solution. An example of these disconnected branches is presented in Fig. 9 for $n = 3$ and $\nu = 30$.

IV. SUMMARY AND DISCUSSION

We have constructed non-Abelian vortices in a $SU(2)$ Chern-Simons-Higgs theory in $2 + 1$ dimensions directly generalizing the Abelian model proposed in [1,2]. These solutions are constructed numerically and sit above the previously known [1,2] Abelian embeddings. Our study is directed in three main directions:

(i) To investigate the dependence of the energies of the non-Abelian vortices on the various parameters characterizing them. Some of these parameters, denoted as p_1, p_2, and α, are the asymptotic values of the various fields describing the model, and since they are not independent of each other—such relations being only seen via the numerical process—we have chosen to focus on the most convenient one, namely p_2, corresponding to the asymptotic value of the electric potential. In particular, the known Abelian embedding solutions possess the value $p_2 = 0$. Physically, the most significant parameter is the Higgs self-interaction strength ν of the symmetry breaking Higgs potential. We find it very convenient and interesting therefore to compare the energies of the non-Abelian vortices with those of the Abelian ones *versus* the coupling ν in the $p_2 = 0$ case (see Fig. 8). We observe that for a range of values of ν the energies of the non-Abelian vortices are lower than those of their Abelian counterparts.

The question of stability is a subtle one. Normally, when a new field is introduced in a classical system, the energy of the system becomes smaller than the original one. Examples of this are the Skyrme model after (diagonal) purely magnetic gauging with $SU(2)$ [26] or with $U(1)$ [27,28], and the $U(1)$ gauging of the Goldstone soliton on $\mathbb{R}^2$ [29]. In both these examples the gauged soliton is topologically stable against its own energy lower bound. On the other hand, when in [27,28] the system supporting a topologically stable soliton of the (purely magnetically) $U(1)$ gauged soliton is augmented with an electric field such that the topological lower bound on the energy of the new system is still bounded only by the lower bound of the purely magnetic system, then it turns out that the energy of the electrically charged system is higher than the purely magnetic charged one. This is not the situation in the case at hand, where the non-Abelian solution is a sphaleron. Accordingly, as observed in Fig. 8, the non-Abelian solution bifurcates[11] from the Abelian one with energy higher than that of the former and then develops a cusp and returns to cross the Abelian branch after which its energy is lower. This may have implications on the stability of some non-Abelian solutions. We have not carried a quantitative stability analysis here since that would go beyond the scope of the present work and will return to this elsewhere soon.

Apart from the question of stability illustrated by the branch structure of Fig. 8, there is another interesting property of the dependence of the energy on the parameters fixing the numerical solution, illustrated by the branch structure of Fig. 9. The latter describes a branch of solutions that is disconnected from the Abelian branch, plotted against the parameter p_2. This phenomenon is strictly one that appears for large values of ν. While the generic solutions are found to be connected to the Abelian embeddings, out of which they grow as their non-Abelianness manifests itself, in the high ν regime there appear disconnected branches. An explanation for this may be the fact that as ν grows, the contribution of the

[11] Bifurcations are a typical occurrence in sphaleron and sphaleronlike solutions, e.g. the bi-sphaleron [30,31] in the standard model that bifurcates from the Klinkhamer-Manton sphaleron.

Higgs potential term must vanish, resulting in the constraint $|\vec{\phi}|^2 = 1$. Thus the dynamics changes from that of a Higgs model to one of a $O(3)$ sigma model.[12] As it happens, the $U(1)$ gauged embedding of this sigma model does indeed support topologically stable solitons [32], so that the energy of the vortices of its $SO(3)$ gauged extensions are also bounded from below, albeit with higher energy than the $SO(2)$ gauged soliton [32]. This passage from a Higgs model to a sigma model has a noteworthy precedent, namely, that of the sphalerons [33] of the standard model in the high Higgs coupling regime, where the limiting solutions describe the bi-sphalerons [30,31] coinciding with the (right) $SU(2)$ gauged techniskyrmions [34] of the $O(4)$ sigma model. In the bi-sphaleron case, this is associated with the excitation of some extra function in the Ansatz of the matter fields. Therefore, we anticipate the possible existence of new solutions of the model considered in this work as well, which would be found beyond the truncation (14).

(ii) Given that the only topological charge in this model is the magnetic charge or the vortex number pertaining to the Abelian subsystem, it is important to find some other global quantity that characterizes the non-Abelian vortices exclusively. This is the angular momentum of the vortex, which in addition to the globally defined magnetic and electric charges pertaining to the Abelian embedding and the energy, provides a global quantity that characterizes the non-Abelian vortex. This quantity differs essentially in the Abelian and the non-Abelian cases (see Eq. (26)) and gives a quantitative measure of the non-Abelianness of the $SU(2)$ vortices.

The value of the angular momentum in the Abelian cases is independent of the coupling constant ν. In that case it is also independent of the energy, whether or not the value of ν is the critical one when the Bogomol'nyi bound is saturated as in [1,2]. In the non-Abelian case by contrast, the angular momentum does depend on the energy. This yields a mass *versus* spin plot (see Fig. 6). Not unexpectedly, it turns out that the only spinless solutions are those with vanishing mass, i.e. trivial solutions with vanishing static energy. For a given value of ν, namely, for a given physical model, this spin-energy behavior is studied again, when varying our favored parameter p_2. We observe that for small values of ν the spin increases with energy, while for large ν there exist regions where the spin decreases with increasing energy. Concerning this, we recall our comment above where it is pointed out that the Higgs model at hand becomes a sigma model in the limit of very large ν.

(iii) Since the solutions we constructed pertain to the model in which the Higgs coupling constant ν is not restricted to the critical Bogomol'nyi value, it is reasonable to inquire about the properties of the Abelian embedding vortices with respect to ν. It turns out that there exist both attractive and repulsive phases of like charged vortices for noncritical values of ν for $\nu < \nu_{\text{critical}}$ and $\nu > \nu_{\text{critical}}$, respectively, with noninteracting vortices for $\nu = \nu_{\text{critical}}$. This is also not surprising and is the same as the situation is for the usual Abelian Higgs vortices.

Finally we comment on the reason for our choice of the simplest $SU(2)$ CS-H model, unlike the $SU(N)$ model of [11] and the more general supersymmetry inspired models employed in [13,14]. In our view, the present $SO_{\pm}(4) \equiv SU_{\pm}(2)$ CS-H model in $2+1$ dimensions is the first member of a hierarchy of the $SO_{\pm}(D+2)$ CS-H model in $D+1$ dimensions. It is planned to study the $D = 4$ and 6 examples in the near future. Also, on general grounds, we expect the basic features of the model considered here to be generic for CS-H configurations with non-Abelian matter fields, and thus to give an idea of the situation in a more general case.

More immediately, we intend to revisit the problem of the present model augmented with the $SU(2)$ YM term, to construct the corresponding non-Abelian vortices numerically. Apart from its intrinsic value, such a numerical investigation would reveal some detailed properties of the analytic results of [35]. The latter work was carried out in the context of giving a rigorous proof of the result of Julia and Zee [36] which states that the vortices of the Abelian Higgs model in $2+1$ dimensions cannot carry electric charge. These authors went further to extend the proof of the Julia and Zee theorem of the Abelian Higgs model, to the $SU(2)$ non-Abelian Higgs model in $2+1$ dimensions, i.e. that the electric charge vanishes also in that case. One would expect that in the limit of the CS term vanishing the (non-Abelian) electric field vanishes.

ACKNOWLEDGMENTS

It is a pleasure to thank Peter Breitenlohner and Valery Rubakov for very helpful discussions concerning the question of stability. We thank Roman Jackiw for having directed us to the results on nonrelativistic non-Abelian vortices. This work is carried out in the framework of Science Foundation Ireland (SFI) Project No. RFP07-330PHY and under Project No. FIS2006-12783-C03-02 of the Spanish Education and Science Ministry. The work of E. R. was supported by the Alexander von Humboldt Foundation.

[12] It is interesting to note that the nonrelativistic $SU(2)$ solitons presented in [7] were also arrived at *via* the $O(3)$ sigma model, which likely correspond to the high Higgs coupling limit of our solutions.

[1] J. Hong, Y. Kim, and P. Y. Pac, Phys. Rev. Lett. **64**, 2230 (1990).
[2] R. Jackiw and E. J. Weinberg, Phys. Rev. Lett. **64**, 2234 (1990).
[3] G. V. Dunne, arXiv:hep-th/9902115.
[4] P. A. Horvathy and P. Zhang, arXiv:0811.2094.
[5] R. Jackiw and S. Y. Pi, Phys. Rev. Lett. **64**, 2969 (1990).
[6] B. Grossman, Phys. Rev. Lett. **65**, 3230 (1990).
[7] G. V. Dunne, R. Jackiw, S. Y. Pi, and C. A. Trugenberger, Phys. Rev. D **43**, 1332 (1991); **45**, 3012(E) (1992).
[8] S. Deser, R. Jackiw, and S. Templeton, Phys. Rev. Lett. **48**, 975 (1982).
[9] H. J. de Vega and F. A. Schaposnik, Phys. Rev. Lett. **56**, 2564 (1986).
[10] C. N. Kumar and A. Khare, Phys. Lett. B **178**, 395 (1986).
[11] H. J. de Vega and F. A. Schaposnik, Phys. Rev. D **34**, 3206 (1986).
[12] K. M. Lee, Phys. Rev. Lett. **66**, 553 (1991).
[13] L. G. Aldrovandi and F. A. Schaposnik, Phys. Rev. D **76**, 045010 (2007).
[14] B. Collie, J. Phys. A **42**, 085404 (2009).
[15] N. S. Manton, Phys. Lett. B **110**, 54 (1982).
[16] M. Shifman and A. Yung, Rev. Mod. Phys. **79**, 1139 (2007).
[17] A. Hanany and D. Tong, J. High Energy Phys. 07 (2003) 037.
[18] R. Auzzi, S. Bolognesi, J. Evslin, K. Konishi, and A. Yung, Nucl. Phys. **B673**, 187 (2003).
[19] M. Shifman and A. Yung, Phys. Rev. D **70**, 045004 (2004).
[20] A. Hanany and D. Tong, J. High Energy Phys. 04 (2004) 066.
[21] L. Jacobs and C. Rebbi, Phys. Rev. B **19**, 4486 (1979).
[22] E. Radu and M. S. Volkov, Phys. Rep. **468**, 101 (2008).
[23] U. Asher, J. Christiansen, and R. D. Russel, Math. Comput. **33** 659 (1979); ACM Trans. Math. Softw. **7** 209 (1981).
[24] B. Hartmann, B. Kleihaus, and J. Kunz, Mod. Phys. Lett. A **15**, 1003 (2000).
[25] B. Kleihaus, J. Kunz, and F. Navarro-Lerida, Phys. Rev. D **69**, 081501 (2004).
[26] Y. Brihaye and D. H. Tchrakian, Nonlinearity **11**, 891 (1998).
[27] B. M. A. Piette and D. H. Tchrakian, Phys. Rev. D **62**, 025020 (2000).
[28] E. Radu and D. H. Tchrakian, Phys. Lett. B **632**, 109 (2006).
[29] K. Arthur, Y. Brihaye, and D. H. Tchrakian, J. Math. Phys. (N.Y.) **39**, 3031 (1998).
[30] Y. Brihaye and J. Kunz, Phys. Rev. D **47**, 4789 (1993).
[31] L. G. Yaffe, Phys. Rev. D **40**, 3463 (1989).
[32] B. J. Schroers, Phys. Lett. B **356**, 291 (1995).
[33] F. R. Klinkhamer and N. S. Manton, Phys. Rev. D **30**, 2212 (1984).
[34] G. Eilam, D. Klabucar, and A. Stern, Phys. Rev. Lett. **56**, 1331 (1986).
[35] J. Spruck and Y. Yang, arXiv:0810.1076.
[36] B. Julia and A. Zee, Phys. Rev. D **11**, 2227 (1975).